

# WIRELESS ACOUSTIC AIRBORNE JET PROPELLER

Akash Roy, Matin Barekatain, Jaehoon Lee, Baptiste Neff, and Eun Sok Kim

Department of Electrical and Computer Engineering, University of Southern California, USA

## ABSTRACT

This manuscript presents airborne jet propulsion by audio sounds and ultrasounds through orifices formed by bulk-micromachining of a silicon wafer. The propeller is integrated with a small, printed circuit board (PCB) with a DC/DC converter, an oscillator, and a power amplifier, all powered by a 100F lithium-ion capacitor to make the propeller operable wirelessly. The peak propulsion force of the wireless propeller is measured to be 63.1 mg (or 618 mN) while the packaged wireless propeller's weight is 10.6 g, including the drive electronics and adapter) when driven by 2.5kHz sinusoidal voltage with 21.4V<sub>pp</sub>. A wired propeller (with 563 mg weight without adapter) is shown to high jump, long jump, wobbly fly, and propel objects. Also, the propeller is shown to work when driven by ultrasounds with a maximum propulsion force of 8.4 mg (82 mN) when driven by 20kHz, 20V<sub>pp</sub> sinusoidal signal. Varying the frequency gradient of the applied sinusoidal pulses is shown to move the propeller to the left or right on demand to reach a specific location.

## KEYWORDS

Airborne Acoustic Propeller, Wireless Acoustic Propeller, Synthetic Air Jet, Ultrasonic Propulsion

## INTRODUCTION

Conventional airborne propulsion based on a jet of fluid requires a jet engine with fuel combustion and is not environment-friendly. On the other hand, acoustic propulsion based on synthetic air jets can be obtained with a set of orifices and an electrically actuated diaphragm that produces sound without any combustion engine. When a thin plate with an array of orifices is placed in front of a vibrating diaphragm, the sound waves (generated by the diaphragm and pass through the orifices) can produce synthetic air jets, which propel the plate and diaphragm [1].

Unlike in liquid, acoustic propulsion is most effectively obtained in the air with synthetic jets in macroscopic [2] and microscopic scales [3]. Airborne acoustic propulsion based on synthetic air jets has been demonstrated in audio [4] and ultrasound frequencies [5]. This paper describes a comparison between an array of orifices fabricated with silicon bulk micromachining and that with a laser cutter, a wireless acoustic propeller, and experimental results with a wired acoustic propeller.

## DESIGN

The acoustic propeller is made with an array of orifices over a 25.2×16.6×0.37mm<sup>3</sup> card-type piezoelectric speaker (APS2513S-T-R, PUI Audio) that weighs 385 mg and has a piezoelectric (and electrically insulated) diaphragm (12×18mm<sup>2</sup>) at its center. The orifices are fabricated either on a silicon wafer (with wet anisotropic etching of silicon) or on a polyester plastic plate with a laser cutter. The orifice

plate is attached to the speaker with a 0.9mm thick double-sided foam tape with an air gap between the two (Fig. 1). We have explored various thicknesses of the substrates along with various orifice dimensions while fixing the orifice pitch to be 1.2mm [5].

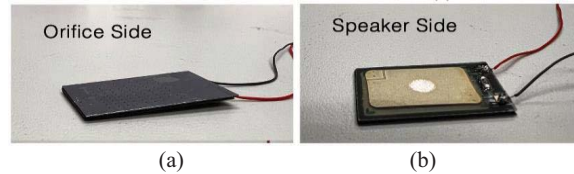


Figure 1: Photos of a bulk micromachined silicon orifice attached to a piezoelectric speaker showing (a) the orifice side and (b) the speaker side.

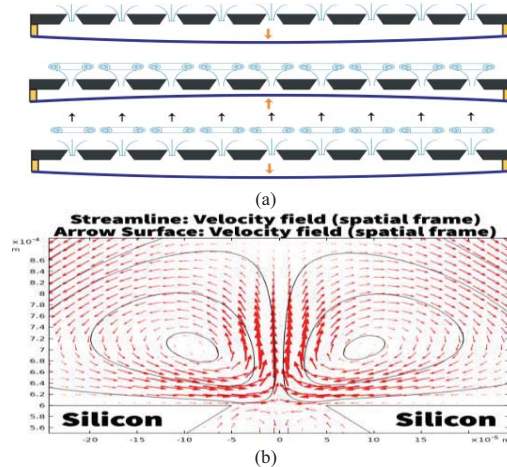


Figure 2: (a) Figures at three different stages, as a diaphragm vibrates to illustrate air-jet generation. (b) Simulated time-averaged velocity field near the orifice on bulk-micromachined silicon due to a vibrating diaphragm below the silicon

A sinusoidal signal applied to the speaker makes the piezoelectric diaphragm vibrate at the signal frequency. As the diaphragm vibrates, it draws in air from the surrounding and pushes it out through the orifices at different stages of the diaphragm bending, as illustrated in Fig. 2b. Depending on the shape and size of the orifice, a vortex ring around the orifice is formed, and propels the orifice plate in the direction opposite to the orifice side. A simulated time-averaged velocity field around an orifice is shown in Fig. 2b.

## ORIFICE FABRICATION

### Laser Micromachining

Polyester sheets of varying thicknesses are used to create circular orifices, which are laser drilled using the LG-500 Jamieson Laser machine. By shining a focused laser beam of a particular intensity onto a solid plate, the laser machine can generate enough heat to melt a specific amount of the plate material, and can produce a via hole.

As the laser energy is more substantial closer to the top surface of the material, the opening produced by the laser is larger at the top, resulting in a nozzle-like structure (Fig. 3a). The side with a larger diameter is made to face the speaker for a more significant propulsion force. Multiple designs of the orifice array have been explored for the highest propulsion with audio and ultrasonic sounds.

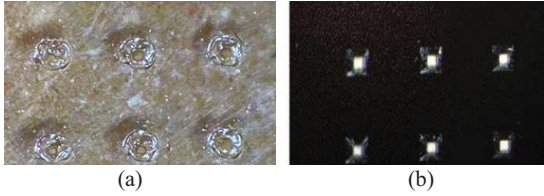


Figure 3: Top view of (a) laser micromachined orifice pattern on a polyester sheet (b) bulk micromachined orifice pattern on a silicon wafer.

### Bulk Silicon Micromachining

Bulk micromachining of silicon is used to create precise, repeatable, and uniform patterns on 200 $\mu\text{m}$  and 400 $\mu\text{m}$  thick silicon substrates (Fig. 3b). A (100) silicon wafer is anisotropically etched with 35% KOH solution at 90 °C to form a square orifice with four slanted (111) sidewalls. The silicon bulk micromachining produces consistent, repeatable orifice patterns and has led to maximum propulsion forces generated in audio and ultrasonic frequencies, generating a maximum force in audio and ultrasonic frequency almost 2.63 times higher [4] and 2.27 times higher [5], respectively, than the maximum with a polyester orifice array.

### MEASUREMENT SETUP

The fabricated propeller is placed on a Mettler Toledo MS104S/03 precision scale with 0.1 mg resolution to measure the propulsion force. The propeller is fixed on a hollow acrylic adaptor with the propeller's orifices facing upward to generate a downward propulsion force, producing a positive weight on the weight scale. The propeller is driven with a Brüel & Kjær power amplifier, which amplifies the signal generated from a function generator to tens of volts. The weight change is recorded with a terminal program in a computer, as an RS232-USB FTDI cable carries the signal from the scale (Fig. 4).

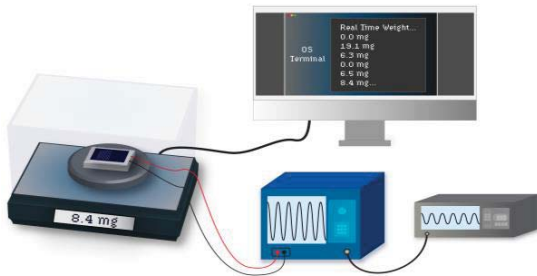


Figure 4: Measurement setup with a signal generator, power amplifier, weight scale, and computer.

## EXPERIMENTAL RESULTS

### Propulsion Force Measurement

The force measurements show that the silicon orifices offer much stronger propulsion than the acrylic orifices

when the speaker is driven with a 20V<sub>pp</sub> sinusoidal signal from a function generator. The device with the 400 $\mu\text{m}$  thick silicon substrate having an array of 9 $\times$ 9 orifices (each of which is 100 $\times$ 100 $\mu\text{m}^2$  in the tapered end) performs best at audio frequencies resulting in a propulsion force of 44.7mg at 2.5kHz. In comparison, the device with the 200 $\mu\text{m}$  thick silicon substrate having an array of 9 $\times$ 9 orifices (each of which is 100 $\times$ 100 $\mu\text{m}^2$  in the tapered end) performs best at ultrasonic frequencies resulting in a force of 8.4mg at 20.5kHz (Fig. 5).

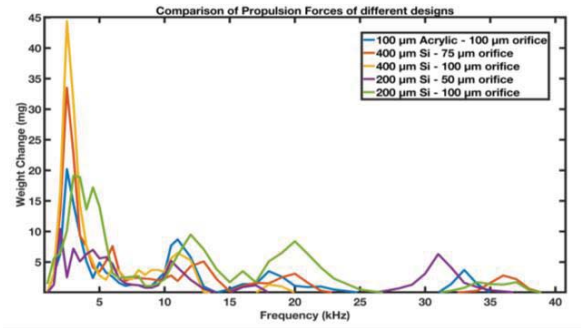


Figure 5: Measured propulsion force at audible and ultrasound frequencies.

Also, the propulsion force measurements indicate that thinner substrates for the orifices produce stronger propulsion in ultrasonic frequencies, while thicker substrates facilitate stronger propulsion in audio frequencies, among the various thicknesses we have explored. The maximum propulsion forces at ultrasonic frequencies obtained by some orifices on silicon substrates are listed in Table 1.

Table 1: Highest ultrasonic propulsion forces with bulk-micromachined orifices (9 $\times$ 9 array) on silicon wafers.

| Silicon Thickness | Orifice Size ( $\mu\text{m}^2$ ) | Propulsion Force | Ultrasonic Frequency |
|-------------------|----------------------------------|------------------|----------------------|
| 400 $\mu\text{m}$ | 100x100                          | 0 mg             | -                    |
| 400 $\mu\text{m}$ | 75x75                            | 3.1 mg           | 20 kHz               |
| 200 $\mu\text{m}$ | 200x200                          | 1.1 mg           | 19 kHz               |
| 200 $\mu\text{m}$ | 100x100                          | 8.4 mg           | 20.5 kHz             |
| 200 $\mu\text{m}$ | 50x50                            | 7.8 mg           | 60 kHz               |

### Experiments to Demonstrate Propulsion

Several experiments have been carried out in audio and ultrasonic frequencies to demonstrate and compare the propulsion forces. The 400 $\mu\text{m}$  thick silicon device with 100 x 100 $\mu\text{m}^2$  is used at audio frequencies and is referred to as D1. The 200 $\mu\text{m}$  thick silicon device with an orifice size of 100 x 100 $\mu\text{m}^2$  is used for further experiments at ultrasound frequencies and is referred to as D2.

#### 1. Demonstration of Offloading

A US quarter coin weighing 5.7 grams is placed on the propeller with its orifice side facing up so the synthetic jet's force can offload the quarter; D1 is operated at 2.4kHz for 1 second at 30V<sub>pp</sub> and D2 at 20.5kHz for 1 second at 48V<sub>pp</sub>. As expected, D1 can offload the quarter more easily than D2, and can completely offload the quarter from the propeller (Fig. 6).



## 2. Demonstration of Load Carrying

Two AA batteries weighing 47.3 grams are placed on D1 with the orifice side facing down for an upward propulsion force. When the propeller is activated with a  $40V_{pp}$  signal of 2.3kHz for 2 seconds, it can move the two batteries by 5.8cm from the initial position (Fig. 7).

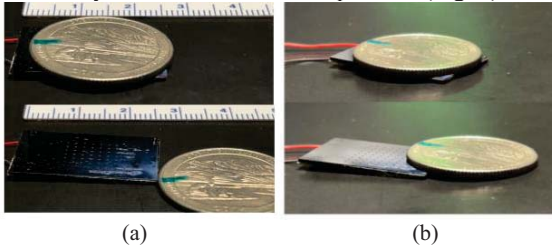


Figure 6: Propellers offloading a US quarter coin with (a) 2.4 kHz,  $30 V_{pp}$  for 1 second and (b) 20.5 kHz,  $48 V_{pp}$  for 1 second.

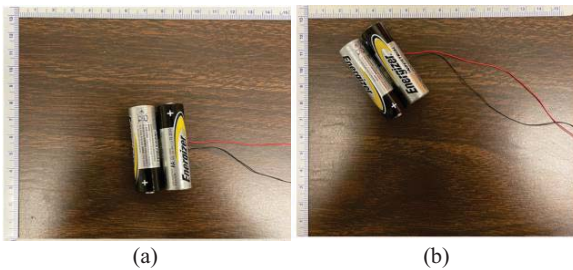


Figure 7: Propeller carrying AA batteries (47.3 g) 5.8 cm when operated at 2.3 kHz with  $40 V_{pp}$  for 2 seconds.

## 3. Demonstration of Object Shooting

A small acrylic cuboid of 70 mg is placed over D1 with its orifice side facing up (Fig. 8a). The propulsion force from D1 is large enough to lift and shoot the object to a peak height of 6.35 cm (Fig. 8b) and a maximum displacement of 15.5 cm (Fig. 8c) when the propeller is operated at 2.4 kHz at  $40V_{pp}$ .

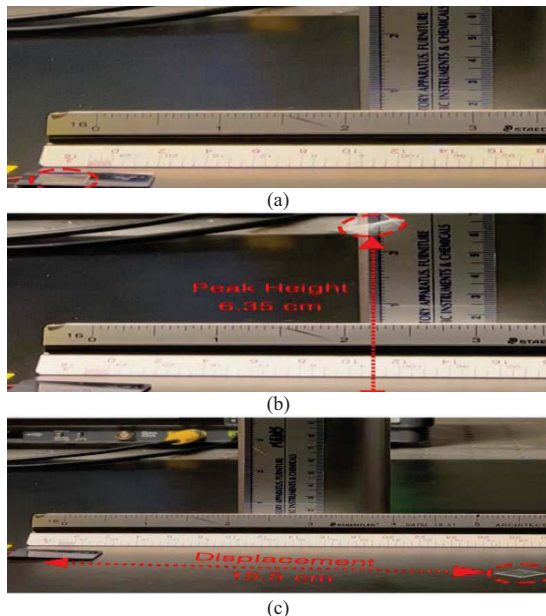


Figure 8: A 70 mg object being propelled with 2.4 kHz,  $40 V_{pp}$  (a) before actuation, (b) at maximum height, (c) just after the object falls.

## 4. Demonstration of Angular Motion

When the propeller is suspended vertically with a string, D1 and D2 can push themselves by  $35.7^\circ$  (Fig. 9a) and  $5.2^\circ$  (Fig. 9b), respectively, when operated with 2.4 and 20.5 kHz, respectively, at  $40 V_{pp}$ .

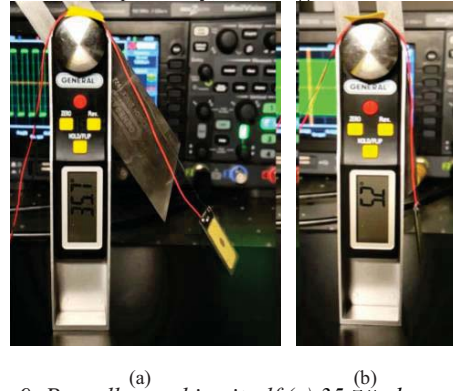


Figure 9: Propeller pushing itself (a)  $35.7^\circ$  when operated with 2.4 kHz at  $40 V_{pp}$  and (b)  $12.8^\circ$  when operated with 20.5 kHz, at  $40 V_{pp}$ .

## Wireless Propeller

The propeller is made *wireless* by integrating it with its drive electronics on a printed circuit board (PCB) and a 100F lithium-ion capacitor. The drive electronics include a Texas Instruments' TPS65131 DC/DC Converter, Analog Devices' LTC1799 Oscillator capable of generating square waves in the range of 1kHz - 33MHz, and a Texas Instruments' THS3095 Power Amplifier (Fig. 10a).

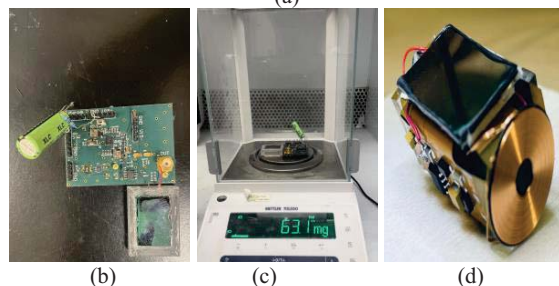
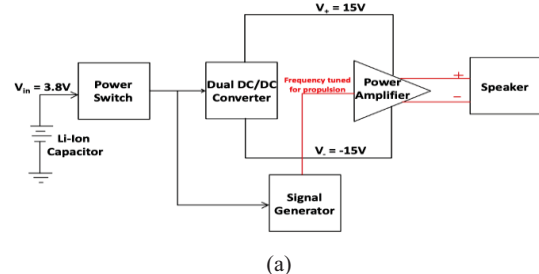


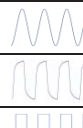
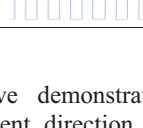
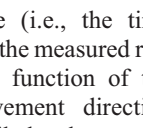
Figure 10: (a) Schematic of the drive electronics (for the wireless propeller) made on a printed circuit board (PCB) and powered by Li-ion capacitor, (b) an unpackaged wireless propeller for testing, (c) measurement setup for the wireless propeller, and (d) a packaged wireless propeller.

The drive electronics are tuned to deliver a  $30V_{pp}$  signal of 2.3kHz to drive the D1 propeller and are powered by a 100F Xeno Energy's XLC-1030 lithium-ion capacitor. The capacitor can provide a maximum of  $3.8V_{DC}$  when fully charged, converted to  $\pm 15V$  with the dual DC/DC converter. A high energy and high-power density lithium-

ion capacitor, not a battery, is used as the propeller needs high instantaneous power since lithium-ion battery has high energy density but low power density. In the case of a supercapacitor, it offers high power density but low energy density and also suffers from self-discharging [6]. Hence, a lithium-ion capacitor is chosen for this application. The total weight of the unpackaged wireless propeller, including the drive electronics, adapter, and capacitor, is 24.8 g.

The drive circuit for the wireless propeller delivers a 2.3 kHz square wave with 21.4 V<sub>pp</sub> to the propeller (powered by a lithium-ion capacitor) (Fig. 10b), which produces a propulsion force of 63.1 mg for about 3 minutes (till the capacitor is discharged) when measured with a setup shown in Fig. 10c. The propulsion force is compared to 47.3 and 68.1 mg obtained by a wired propeller which is driven by a sine wave and a square wave function generator, respectively (Table 2). The wireless propeller with all the same components is further miniaturized, via flexible PCB, into a 10.6 g packaged version (Fig. 10d).

Table 2: Measured propulsion forces of the propeller with 100µm orifice on 400µm thick silicon when driven by 21.4V<sub>pp</sub> at 2.5kHz

| Signal Source                            | Propulsion Force | Observed Waveform   |
|--|------------------|---|
| Sine Wave Function Generator             | 44.7 mg          |    |
| Drive Electronics for Wireless Propeller | 63.1 mg          |   |
| Square Wave Function Generator           | 68.1 mg          |  |

### Controlled Propeller Movement

With a wired propeller, we have demonstrated electrical controllability of the movement direction by varying the applied frequency in time (i.e., the time gradient of the frequency). Table 3 shows the measured rate of change of movement direction as a function of the applied frequency gradient. The movement direction depends on the frequency gradient, likely due to an imbalance in the air jets generated by the orifice array.

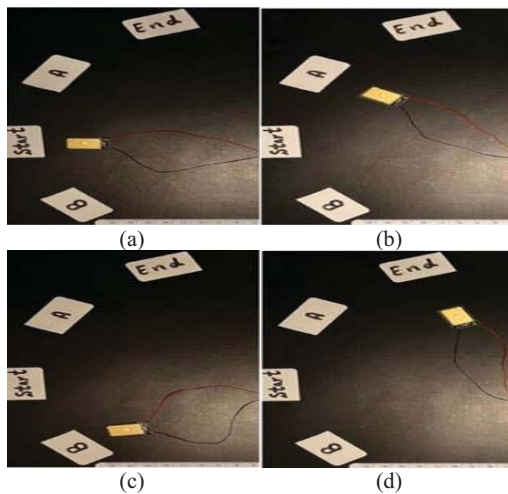


Figure 11: Photos showing the controlled movements of the propeller under 21 kHz, 40 V<sub>pp</sub> from (a) “Start” to (b) “A” to (c) “B” to (d) “End”.

As we manually adjust the frequency gradient on the Function Generator used to generate sine waves, we obtain a controlled movement from “Start” to “End” via “A” and “B,” as shown in Fig. 11.

Table 3: Measured propeller’s movement direction vs applied frequency gradient.

| Frequency Gradient    | Directional Rate of Movement |
|-----------------------|------------------------------|
| 0.2 kHz/sec for 2 sec | 6.2 °/sec                    |
| 0.4 kHz/sec for 2 sec | 11.4 °/sec                   |
| 0.6 kHz/sec for 2 sec | 19.4 °/sec                   |
| 0.8 kHz/sec for 2 sec | 15.25 °/sec                  |
| 0.9 kHz/sec for 2 sec | 10 °/sec                     |
| 1 kHz/sec for 2 sec   | 4 °/sec                      |

### SUMMARY

This paper presents experimental results on airborne acoustic propellers with orifice arrays made with laser and bulk silicon micromachining. The measured propulsion forces show that the propellers with the orifices made on a silicon substrate with anisotropic silicon etching produce substantially higher propulsion forces, both in audio and ultrasonic frequencies, than the ones made with acrylic orifices fabricated by a laser cutter. Various experiments have been carried out to show the versatility (and electrical controllability) of acoustic propulsion. Also, a wireless propeller with the drive electronics and its power source (a lithium-ion capacitor) is shown to produce a maximum propulsion force of 618 mN.

### ACKNOWLEDGEMENTS

This paper is based on the work supported by National Science Foundation under grant ECCS-2017926.

### REFERENCES

- [1] B. L. Smith and A. Glezer, “The Formation and Evolution of Synthetic Jets,” *Physics of Fluids*, vol. 10, no. 9, pp. 2281–2297, 1998.
- [2] U. Ingård and S. Labate, “Acoustic Circulation Effects and the Nonlinear Impedance of Orifices,” *The Journal of the Acoustical Society of America*, vol. 22, no. 2, pp. 211–218, 1950.
- [3] S. G. Sawant, B. George, L. S. Ukeiley, and D. P. Arnold, “Microfabricated Electrodynamic Synthetic Jet Actuators,” *Journal of Microelectromechanical Systems*, vol. 27, no. 1, pp. 95–105, 2018.
- [4] Y. Tang and E. S. Kim, “Acoustic Propeller Based on Air Jets from Acoustic Streaming,” *2019 Transducers & Eurosensors XXXIII*, Berlin, Germany, 2019, pp. 2068-2071
- [5] H. Liu, A. Roy, Y. Tang, M. Barekatin and E.S. Kim, “Ultrasonic Air-Borne Propulsion Through Synthetic Jets,” *Solid-State Sensor and Actuator Workshop*, Hilton Head Island, SC, June 5 - 9, 2022, pp. 226 - 229.
- [6] J. Lee and E.S. Kim, “Wireless and Stand-Alone Submarine Propeller Based on Acoustic Propulsion,” *Solid-State Sensor and Actuator Workshop*, Hilton Head Island, SC, June 5 - 9, 2022, pp. 230 - 233.

### CONTACT

\*Akash Roy, tel: +1-323-541-8060; akashroy@usc.edu